

## Performance evaluation of a three dimensional intensity probe

Hideo Suzuki,\* Shun Oguro,\* Masazou Anzai,\* and Takahiko Ono\*\*

\**Ontek R & D Co., Ltd.,*

*1-16-1, Hakusan, Midori-ku, Yokohama, 226 Japan*

\*\**Ono Sokki Co., Ltd.,*

*1-16-1 Hakusan, Midori-ku, Yokohama, 226 Japan*

*(Received 26 August 1994)*

A three dimensional intensity probe using four microphones is proposed. Four microphones are placed at apexes of a regular tetrahedron. One is placed in the front and three others consisting a vertical regular triangle are in the back. The microphones are attached at the tips of parallel thin tubes. The microphone arrangement is not the conventional face to face type. The aim of this type of microphone arrangement is to design a sound intensity probe with a simple structure, which is essential for reducing the diffraction problem. Algorithms for three dimensional intensity components from cross spectra are given as well as for leakage components. Measurements of sensitivity characteristics in an anechoic room using two types of probes with 60 mm and 20 mm microphone separations show that sensitivity fluctuations are small enough (less than 1 dB) for the practical application of the sound intensity method. The leakage errors of approximately 5% (-13 dB) seem also acceptable. The measurement results indicate that sensitivity and leakage errors will become smaller if a more ideal plane wave field in an anechoic room is achieved.

Keywords: Sound intensity, Probe, Three dimensional

PACS number: 43. 85. Fm

### 1. INTRODUCTION

The sound intensity method is frequently used for the purposes of noise evaluation and reduction. The most common sound intensity probe is a one dimensional (1-D) p-p type probe, in which two identical pressure microphones are placed on one axis with a finite separation. Since the sound intensity is a vector, it becomes necessary in some cases to measure components in three dimensions (3-D). In these cases, the measurement must be repeated three times at the same point. Consequently, the measurement time becomes long causing significant problems in some applications of the sound intensity method. For example, a combustion engine with an extremely high rotating speed can be run only for a short time, which may be too

short for the 3-D sound intensity measurement using a 1-D probe. Or the same engine with a normal rotating speed may change its operating condition while the sound intensity is being measured if the measurement time is long. These problems may be solved if a 3-D probe reduces the measurement time to one third. Other advantages of the 3-D probe are that it can be applied to the analysis of transient sounds and that the direction of the sound source is graphically indicated in real time.

For the 3-D intensity measurement, at least four microphones must be placed in the 3-D space. Three 1-D probes may be combined together making a single 3-D probe. In this case 6 microphones are used. Other methods are to use four microphones placed at apexes of a tetrahedron. In the next section, microphone arrangements for 3-D intensity

probes will be discussed. A specific microphone arrangement using four microphones is proposed. In the following sections, algorithms for the sensitivity and leakage characteristics and some results of performance evaluation of the proposed 3-D probe will be described.

## 2. VARIOUS MICROPHONE ARRANGEMENTS FOR 3-D PROBES

A simple extension of the 1-D probe to a 3-D probe is to use three 1-D probes.<sup>1)</sup> Figure 1 shows the microphone arrangement for this case. Six microphones are placed at the centers of the six planes of a cube. Three microphone pairs 1-2, 3-4, and 5-6, which share the same origin, are used for the measurement of the  $x$ ,  $y$ , and  $z$  components of the sound intensity, respectively. A symmetry of the microphone arrangement is an advantage of this type of probe. A disadvantage of this probe is that the structure of the probe becomes clumsy and may disturb the sound field. Another disadvantage is a use of a rather large number of microphones making the probe and a processor costly.

At least two microphone arrangements using four microphones are possible. Figure 2 shows one of them, in which four microphones are placed at the apexes of a regular tetrahedron.<sup>2)</sup> The apexes of the tetrahedron coincide with four apexes of the cube as shown in Fig. 1 and the  $x$ ,  $y$ , and  $z$  axes are taken by the same way as in Fig. 1. The pressure at microphone 1 in Fig. 1 is obtained by the average of the output of microphones 1 and 2 in Fig. 2. Similarly, other five combinations of two microphones out of the four in Fig. 2 give pressures at five other microphone positions in Fig. 1. The

calculation of the intensity are almost the same as the six microphone probe. This arrangement of the microphones has a symmetry with respect to the three ( $x$ ,  $y$ , and  $z$ ) axes in the sense that the four microphones are used with an equal weighting. In this arrangement, however, the microphone positions do not give a direct image of the probe direction causing a difficulty in practical usage.

Figure 3 shows a new arrangement of four microphones which are placed at the apexes of a regular tetrahedron as in Fig. 2. However, the  $x$ ,  $y$ , and  $z$  axes are taken in a different way.<sup>3)</sup> The  $z$  (rear/front) axis is taken on a line connecting microphone 4 and the center of the gravity of the tetrahedron. The  $x$  (left/right) and  $y$  (bottom/top) axes are taken as horizontal and vertical lines crossing the center of the gravity, respectively. Since this arrangement

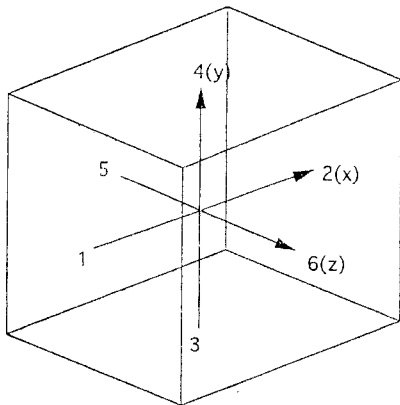


Fig. 1 Six microphone arrangement for a 3-D probe proposed by P. Rasmussen.

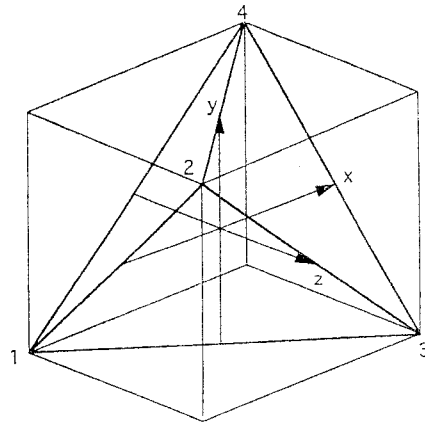


Fig. 2 Four microphone arrangement for a 3-D probe proposed by Santos *et al.*

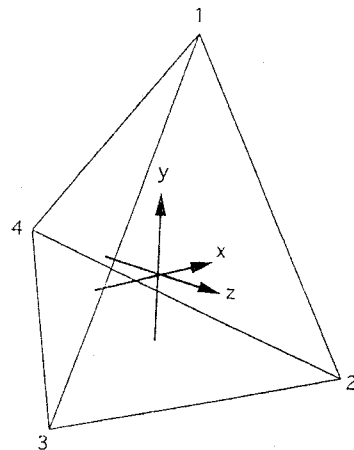


Fig. 3 Four microphone arrangement for a 3-D probe proposed by Suzuki *et al.*

does not have the symmetry as in Fig. 2, the three intensity components are obtained using four microphone outputs with different weights. However, as Fig. 6 shows, this type of probe can be easily aimed at a sound source with a desired orientation. The aim of this type of microphone arrangement is to design a sound intensity probe with a simple structure, which is essential for reducing the diffraction problem. The use of four microphones instead of six is an advantage for the simplicity and cost of the amplifier and processor.

### 3. DERIVATION OF FORMULAE FOR 3-D SOUND INTENSITY COMPONENTS

Two basic assumptions to derive an algorithm to obtain the  $x$ ,  $y$ , and  $z$  components of the sound intensity are as follows:

(1) The pressure at the center of the gravity of the tetrahedron is given by the average of the pressures at the four apexes of the tetrahedron.

$$P_0 = (P_1 + P_2 + P_3 + P_4)/4 \quad (1)$$

where  $P_i$  is the pressure spectrum (rms amplitude as a function of frequency) at the  $i$ -th apex.

(2) The particle velocity components  $V_i$  at the gravity center in the direction from each apexes to the gravity center are obtained using  $P_i$  and  $P_0$ .

$$V_i = -(P_i - P_0)/j2\pi f\rho a \quad (i=1, 2, 3, \text{ and } 4) \quad (2)$$

where  $f$  is the frequency,  $\rho$  is the air density, and  $a$  is the distance from the gravity center to the apexes.

From the geometry of the tetrahedron, relations between  $V_i$  and  $V_x$ ,  $V_y$ , and  $V_z$  are given, respectively, by

$$V_1 = +\frac{2\sqrt{2}}{3}V_x + \frac{1}{3}V_z \quad (3)$$

$$V_2 = \frac{\sqrt{2}}{3}V_x - \frac{\sqrt{2}}{3}V_y + \frac{1}{3}V_z \quad (4)$$

$$V_3 = -\frac{\sqrt{2}}{\sqrt{3}}V_x - \frac{\sqrt{2}}{3}V_y + \frac{1}{3}V_z \quad (5)$$

and

$$V_4 = -V_z \quad (6)$$

where  $V_x$ ,  $V_y$ , and  $V_z$  are the  $x$ ,  $y$ , and  $z$  components (frequency spectrum) of the particle velocity at the gravity center. By solving the above set of simultaneous equations,  $V_x$ ,  $V_y$ , and  $V_z$  are given, respectively, by

$$V_x = -\frac{\sqrt{3}}{2\sqrt{2}}(V_2 - V_3) \quad (7)$$

$$V_y = -\frac{1}{2\sqrt{2}}(2V_1 - V_2 - V_3) \quad (8)$$

and

$$V_z = -\frac{1}{4}(V_1 + V_2 + V_3 - 3V_4) \quad (9)$$

The active sound intensity in the  $x$  direction, for example, is given by

$$AI_x = \text{Re}(P^* V_x) \quad (10)$$

Rewriting Eq. (10) using Eq. (7) and Eq. (2),  $AI_x$  is given by

$$AI_x = \frac{-3}{2\pi f\rho d} \frac{1}{12} \text{Im}(G_{35} - G_{24} - 2G_{23} + G_{12} - G_{13}) \quad (11)$$

where  $d$  is the length of the sides of the tetrahedron ( $d = (2\sqrt{2}/\sqrt{3})a$ ) and  $G_{ij}$  is the one-sided cross spectrum between the pressures at the  $i$ -th and  $j$ -th apexes. Similarly,

$$AI_y = \frac{-3}{2\pi f\rho d} \frac{\sqrt{3}}{36} \text{Im}(G_{34} + G_{24} - 2G_{14} - 3G_{12} - 3G_{13}) \quad (12)$$

and

$$AI_z = \frac{-3}{2\pi f\rho d} \frac{\sqrt{2}}{6\sqrt{3}} \text{Im}(-G_{34} - G_{24} - G_{14}) \quad (13)$$

### 4. DISCUSSION OF ERRORS

Errors due to the approximations given by Eqs. (1) and (2) are discussed here. When a plane wave propagates in the  $x$  direction, the intensity components in the  $x$ ,  $y$ , and  $z$  directions are given, respectively, by

$$AI_{xx} = \frac{P^2}{\rho c} \frac{1}{2} \left(1 + \cos \frac{\pi d}{\lambda}\right) \sin\left(\frac{\pi d}{\lambda}\right) \Big/ \frac{\pi d}{\lambda} \quad (14)$$

$$AI_{xy} = 0 \quad (15)$$

and

$$AI_{xz} = 0 \quad (16)$$

where  $\lambda$  is the wavelength. Similarly, for plane waves that propagate in the  $y$  and  $z$  directions, the intensities in the  $x$ ,  $y$ , and  $z$  directions are given, respectively, by

$$AI_{yx} = 0 \quad (17)$$

$$AI_{yy} = \frac{P^2}{\rho c} \frac{1}{12} \left\{ \left(1 + 2 \cos \frac{\pi d}{\sqrt{3}\lambda}\right) \sin\left(\frac{\pi d}{\sqrt{3}\lambda}\right) \Big/ \frac{\pi d}{\sqrt{3}\lambda} + 9 \sin\left(\frac{\sqrt{3}\pi d}{\lambda}\right) \Big/ \frac{\sqrt{3}\pi d}{\lambda} \right\} \quad (18)$$

$$AI_{yz} = \frac{P^2}{\rho c} \frac{-1}{3\sqrt{2}} \left( 1 - \cos \frac{\pi d}{\sqrt{3}\lambda} \right) \cdot \sin \left( \frac{\pi d}{\sqrt{3}\lambda} \right) / \frac{\pi d}{\sqrt{3}\lambda} \quad (19)$$

and

$$AI_{zx} = 0 \quad (20)$$

$$AI_{zy} = 0 \quad (21)$$

$$AI_{zz} = \frac{P^2}{\rho c} \sin \left( \frac{2\sqrt{2}\pi d}{\sqrt{3}\lambda} \right) \quad (22)$$

If  $d/\lambda \ll 1$ , all the diagonal components are equal to  $P^2/\rho c$  as expected. There exists a non-zero off-diagonal component ( $=AI_{yz}$ ). The diagonal and off-diagonal components are considered as the sensitivity and leakage error characteristics, respectively. Frequency characteristics of these components normalized to  $P^2/\rho c$  are shown in Fig. 4. Magnitudes of sensitivity reduction of the diagonal components

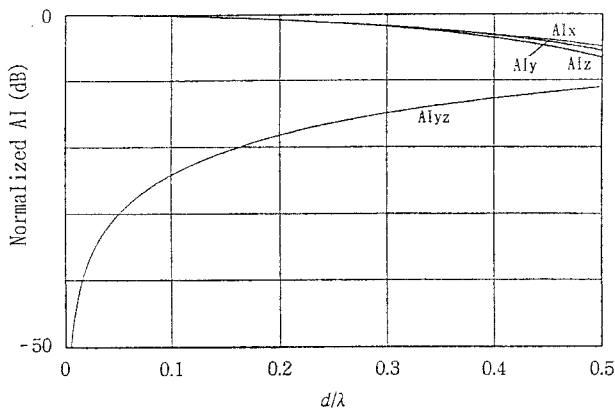


**Fig. 4** Theoretical sensitivity and leakage errors for the proposed 3-D intensity probe.

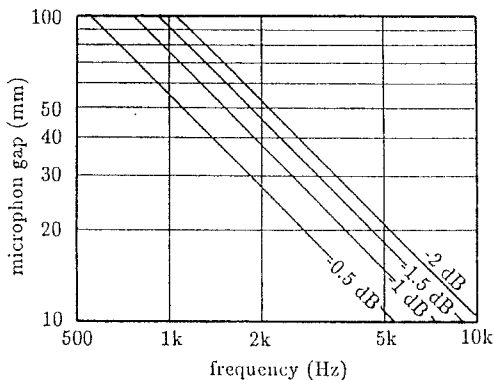


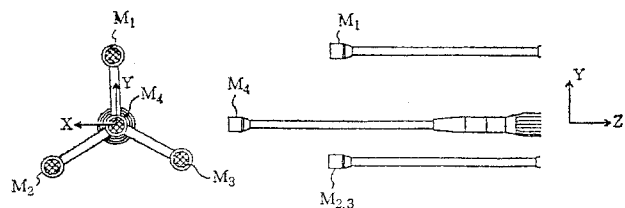
**Fig. 5** Sensitivity error vs microphone separation.

are within 1 dB in the range  $d/\lambda < 0.2$ . Also  $AI_{yz}$  is more than 20 dB below  $P^2/\rho c$  in the range  $d/\lambda < 0.16$ . Therefore, errors due to the approximations given by Eqs. (1) and (2) are negligible as far as  $d/\lambda < 0.16$ . Figure 5 shows relations between the microphone separation ( $d$ ) and sensitivity reduction of  $-0.5$ ,  $-1.0$ ,  $-1.5$ , and  $-2.0$  dB. The results indicate that the microphone separation of 60 mm for the 3-D probe is equivalent to 50 mm of the 1-D probe. If a 1 dB error is allowed, the upper limiting frequency of the 60 mm probe is approximately 1.2 kHz. There is a compensation method of extending this frequency for a 3-D intensity probe.<sup>4)</sup>

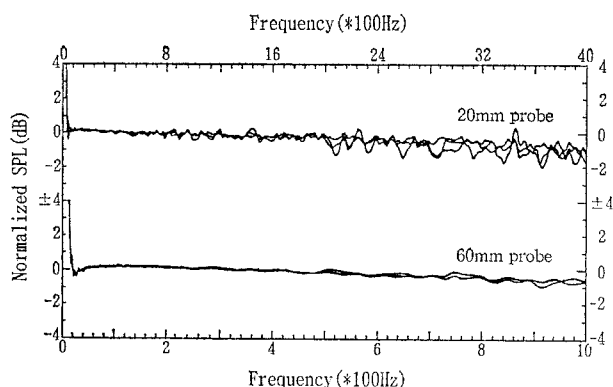
### 5. PERFORMANCE EVALUATION OF THE PROPOSED 3-D PROBE

Figure 6 shows an actual design of the probe with the proposed microphone arrangement. Each microphones with a 7 mm diameter are placed at the top of a tube with a 4 mm diameter. The sensitivity and leakage characteristics of this probe were measured in an anechoic room. The intensity probe was placed 1 m in front of a loudspeaker in the anechoic room. The sensitivity and leakage characteristics were measured for three cases when the  $x$ ,  $y$ , or  $z$  axes of the probe coincides with the loudspeaker axis.

Figure 7 shows normalized pressure responses of the intensity probes (Eq. (1)) with 60 mm and 20 mm microphone separations. A pressure output of a 1/4 inch measuring microphone placed at the same position as the intensity probe (gravity center of the tetrahedron) was used for the pressure response normalization. The pressure sensitivity decreases as the frequency rises (approximately 0.7 dB at 1 kHz for the 60 mm probe and 1 dB at 4 kHz for the 20 mm probe). The pressure sensitivity reduction is common for both 1-D and 3-D probes. For a propagating plane wave field, when an average pressure is obtained from two or more pressure signals



**Fig. 6** An actual design of the proposed 3-D intensity probe.



**Fig. 7** Pressure responses of the proposed 3-D probe with 60 mm and 20 mm microphone separations.

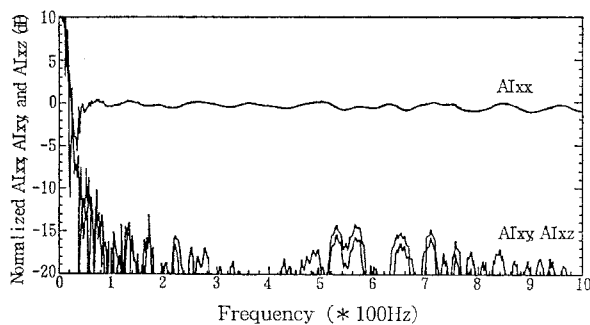


**Fig. 8** Sensitivity and leakage characteristics of a probe with 60 mm separation for a wave travelling in the *x* direction.

with some phase difference, the average pressure is always smaller than the individual pressure level. The fluctuations of the pressure is less than 0.5 dB and 1 dB for 60 mm and 20 mm probes, respectively. Candidates for the causes of the fluctuation are the reflections in the anechoic room and the diffraction due to the intensity probe. The latter may be dominant in the high frequency region.

Figures 8–10 and 11–13 show the normalized intensity and leakages of the 60 mm and 20 mm probes, respectively, for the plane propagating waves coming from negative *x*, *y*, and *z* directions. It is assumed that the true intensity level at the measurement point (gravity center of the tetrahedron) is equal to  $P^2/\rho c$  where  $P^2$  is the pressure squared measured by the 1/4 inch microphone. The measured sensitivity characteristics (or sound intensity normalized to  $P^2/\rho c$ ) for *x*, *y*, and *z* directions are almost identical for the 60 mm probe and very similar for the 20 mm probe, indicating that the

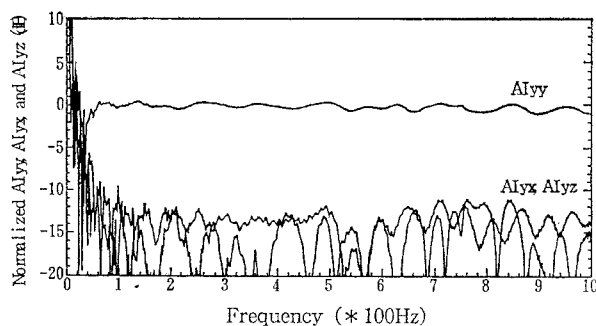


**Fig. 9** Sensitivity and leakage characteristics of a probe with 60 mm separation for a wave travelling in the *y* direction.

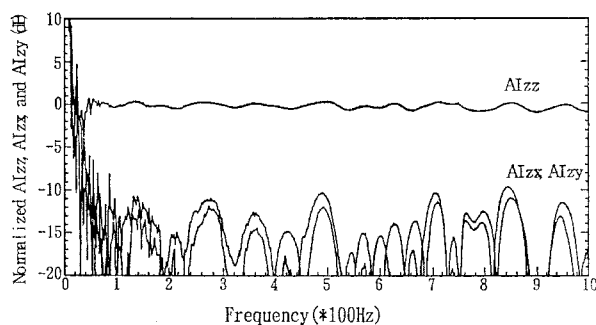


**Fig. 10** Sensitivity and leakage characteristics of a probe with 60 mm separation for a wave travelling in the *z* direction.

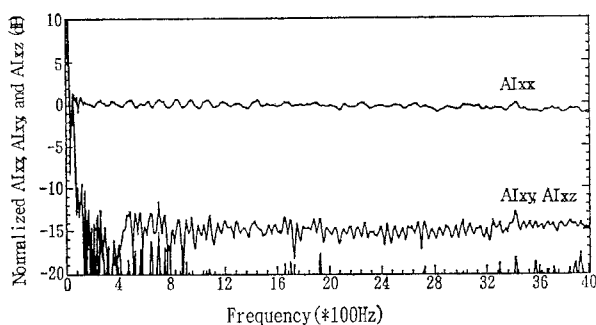


**Fig. 11** Sensitivity and leakage characteristics of a probe with 20 mm separation for a wave travelling in the *x* direction.

main cause of the sensitivity fluctuation is probably that the sound field is not an ideal plane propagating wave. If the fluctuation is caused by the diffraction around the probe, irregularities may be different with different probe orientations relative to the incident wave. It is also expected that the effect of the phase characteristic differences among micro-

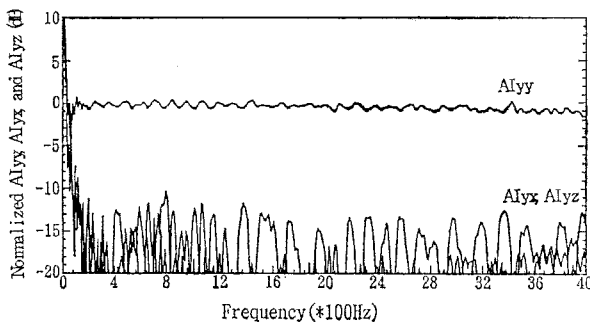


**Fig. 12** Sensitivity and leakage characteristics of a probe with 20 mm separation for a wave travelling in the  $y$  direction.

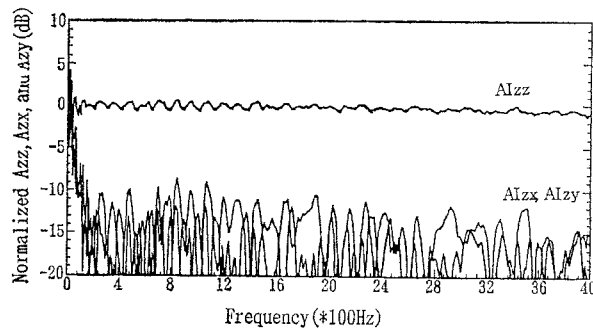


**Fig. 13** Sensitivity and leakage characteristics of a probe with 20 mm separation for a wave travelling in the  $z$  direction.

phones are very small since they are calibrated by use of a specially designed calibrator. The sensitivity characteristics show that the 60 mm and 20 mm probe can be used in the frequency range below 4 kHz and 4 kHz, respectively.

The leakage characteristics for the 60 mm and 20 mm probes are also shown in Figs. 8–10 and 11–13, respectively. Roughly speaking, the leakage levels are approximately  $-13$  dB (5%). Some are lower and some others are higher than this. It seems that the leakage levels shown in Figs. 8–13 are small enough for a practical use of the proposed 3-D intensity probe. The strong frequency dependent nature of the leakage indicates that the sound field is the main cause of the problem as in the case of the sensitivity characteristics measurement. It should be reminded that the measurement of leakage is in general very difficult. If the probe orientation is  $3^\circ$  off the axis, there is a 5% leakage. There is no guarantee that the sound energy flows along the geometrical axis of the loudspeaker. Even in a

high quality anechoic room, there are reflections from reflecting objects in the room that are necessary for the measurement setup. Considering all these causes, it is expected that the true leakage errors are smaller than those shown in Figs. 8–13.

## 6. CONCLUSION

A new type of three dimensional sound intensity probe was introduced. It uses four microphones, which are located at the apexes of a regular tetrahedron. The minimum number of microphones for a three dimensional intensity measurement makes it possible to design a probe with a simple structure, which is essential for reducing the diffraction problem. Four channel signals of the probe can be easily processed with a general purpose four channel FFT analyzer. Formulae to calculate  $x$ ,  $y$ , and  $z$  components and leakage errors for a plane wave that travels along each axes were also given. A probe with the proposed configuration was built and the sensitivity and leakage characteristics were measured. Measured sensitivity characteristics coincide with predictions given by the formulae. The measurement also shows that a probe with 20 mm microphone separation can be used in the frequency range of up to 4 kHz without a diffraction problem. Measured leakage errors are approximately  $-13$  dB (5%), which may be low enough for a practical use of sound intensity method. It is also suspected that a cause of these leakages is the imperfectness of the sound field.

Sensitivity and leakage errors for the analysis of the sound field near the source by use of the three dimensional intensity probe will be discussed in the near future.

## REFERENCES

- 1) G. Rasmussen, "Measurement of vector sound fields," Proc. 2nd Int. Congr. Acoustic Intensity, 53–58 (1985).
- 2) L. M. S. Santos, C. C. Rodrigues, and L. Bento Coelho, "Measuring the three-dimensional acoustic intensity vector with a four-microphone probe," Proc. Inter-Noise 89, 965–968 (1989).
- 3) H. Suzuki, M. Anzai, S. Oguro, and T. Ono, "A three-dimensional sound intensity probe," *J. Acoust. Soc. Am.* **91**, 4, Pt. 2, 2370 (1992).
- 4) H. Suzuki, S. Oguro, M. Anzai, and T. Ono, "A sensitivity compensation method for a three dimensional intensity probe," Proc. Inter-Noise 94, 1963–1966 (1994).